RESEARCH ARTICLE

NANO · MICRO small
www.small-journal.com

# An Outer Membrane-Inspired Polymer Coating Protects and Endows *Escherichia coli* with Novel Functionalities

*Andrea Belluati,* Iain Harley, Ingo Lieberwirth, and Nico Bruns**

**A bio-inspired membrane made of Pluronic L-121 is produced around *Escherichia coli* thanks to the simple co-extrusion of bacteria and polymer vesicles. The block copolymer-coated bacteria can withstand various harsh shocks, for example, temperature, pressure, osmolarity, and chemical agents. The polymer membrane also makes the bacteria resistant to enzymatic digestion and enables them to degrade toxic compounds, improving their performance as whole-cell biocatalysts. Moreover, the polymer membrane acts as an anchor layer for the surface modification of the bacteria. Being decorated with $\alpha$-amylase or lysozyme, the cells are endowed with the ability to digest starch or self-predatory bacteria are created. Thus, without any genetic engineering, the phenotype of encapsulated bacteria is changed as they become sturdier and gain novel metabolic functionalities.**

## 1. Introduction

In nature, most uni- and multicellular organisms comprise cells whose membranes are surrounded by additional protective layers, generically named cell wall, found in most prokaryotes, fungi, algae, and plants. The cell wall provides structural support and resistance from external stressors, regardless of its diverse chemical structures.[1] Synthetic coatings composed of multiple protective layers have been extensively developed, for instance, as delivery devices for encapsulated small molecules and particles.[2] A natural progression was to encapsulate—or coat—living cells within natural and/or synthetic materials, affording protection and separation from the outside environment.[3] Cell encapsulation refers to a broad range of immobilization techniques that entrap cells within well-defined matrixes, often overlapping with cell coating.[4] It provides cytoprotection,[3a] and can be used for cell delivery,[5] and to co-culture different strains and species for industrial applications.[6] These techniques, for the greatest part, rely on the encapsulation of several cells per object, be it a capsule, hydrogel, droplet, and so forth, entrapping the equivalent of small cellular populations or biofilms in the case of bacteria. Albeit with obvious advantages, such as a higher payload per unit and ease of recovery, the main shortcoming of multi-cell encapsulation is that of any multicellular organism, where a lower surface/volume ratio decreases the mass transfer rate for metabolites.[7] To this end, single-cell encapsulation, developed initially as a way to segregate and analyze heterogeneous cell populations and to improve cell delivery systems,[8] offers an opportunity to link the optimal compound exchange provided by the high surface-to-volume ratio with the physical enhancement that cell encapsulation can provide. In this regard, both animal cells and eukaryotic microbes (e.g., yeasts, diatoms) have been encapsulated within droplets or vesicles,[9] polymeric microgels,[8] within capsules made of polyphenols,[4] and in inorganic compounds.[10] Single prokaryotes have also been encapsulated in a variety of materials: mainly polymers,[11] organic–inorganic composites,[11f,12] and graphene,[13] to improve their utility both as delivery vectors and whole-cell catalysts, a technique known as single-cell nanoencapsulation (SCNE). A peculiar strategy is to co-extrude erythrocytes with *Escherichia coli*, exploiting the self-assembly of the phospholipid membrane of the erythrocytes to reform an additional membrane around the bacteria, allowing them to act as stealthy, living therapeutics.[14] However, this approach relies on unstable, immunogenic phospholipid membranes of biological origin, limiting the spectrum of applications. We thus turned our attention to amphiphilic block copolymers as synthetic mimics of phospholipids, which offer additional physical resistance, chemical versatility, and biocompatibility.[15] We selected the well-known, inexpensive, amphiphilic triblock copolymer Pluronic L-121 (PL121, poly(ethylene glycol)-*block*-poly(propylene glycol)-*block*-poly(ethylene glycol), $PEG_5$-*b*-$PPG_{62}$-*b*-$PEG_5$)[12a] to form cell-sized giant unilamellar vesicles (GUVs)[16] that were extruded together with *E. coli* through a track-etched membrane creating an additional thin block copolymer membrane around the bacteria.

A. Belluati, N. Bruns
Department of Chemistry and Centre for Synthetic Biology
Technical University of Darmstadt
Peter-Grünberg-Straße 4, 64287 Darmstadt, Germany
E-mail: andrea.belluati@tu-darmstadt.de; nico.bruns@tu-darmstadt.de
A. Belluati, N. Bruns
Department of Pure and Applied Chemistry
University of Strathclyde
295 Cathedral Street, Glasgow G1 1XL, UK
I. Harley, I. Lieberwirth
Department of Physical Chemistry of Polymers
Max Planck Institute for Polymer Research
Ackermannweg 10, 55128 Mainz, Germany

The ORCID identification number(s) for the author(s) of this article can be found under https://doi.org/10.1002/smll.202303384



**DOI: 10.1002/smll.202303384**

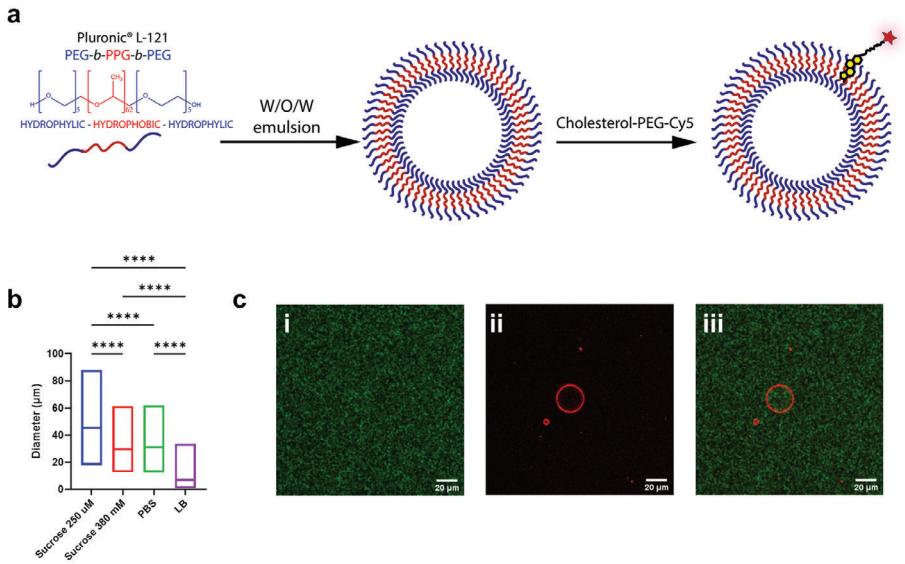


**Figure 1.** a) Schematic of the production of PL121 GUVs and their fluorescent tagging with cholesterol-PEG$_4$-Cy5. b) Mean distribution of the resulting GUVs in different outer water phases (±S.D., $n \geq 50$ GUVs). c) Representative confocal laser scanning microscopy (CLSM) micrograph of GUVs (i) fluorescein; ii) Cy5-labeled membrane; iii) overlay). ****: $p < 0.0001$.

This membrane not only increased the cell viability in a wide variety of physicochemical stresses but also became a new anchor layer to decorate the bacteria with clickable moieties, effectively modifying their surface without any additional covalent bonds to the molecules on the cell. The surface-modified bacteria could be functionalized with bio-orthogonal exoenzymes (α-amylase, lysozyme) that altered their phenotype without genetic manipulation. Our design creates robust and versatile bacteria to be applied in white and red biotechnology (e.g., biocatalysis for industrial scopes for the former or delivery of therapeutics for the latter).

## 2. Results and Discussion

### 2.1. Single-Cell Encapsulation

To develop an easy and adaptable encapsulation method, PL121 was chosen as the membrane-building polymer. The amphiphilic triblock copolymer forms GUVs via a simple water/oil/water emulsion pipetting protocol.[17] After the solvent evaporation, the GUVs can be decorated with cholesterol-PEG$_4$-Cy5, which inserts efficiently into their membrane and allows their imaging (**Figure 1**a).[18] Different outer aqueous phases (sucrose solutions, phosphate-buffered saline (PBS), cell culture medium) were tested, and all of them yielded GUVs. Their average size decreased as the salt content increased, with the growth medium Luria-Bertani (LB) yielding GUVs of a mean diameter <10 µm (Figure 1b). Mixing the formed vesicles with fluorescein confirmed that the membrane is intrinsically permeable to hydrophilic molecules in the range of a few hundred Da (Figure 1c).[19]

We thus proceeded to mechanically extrude the bacteria and GUVs together in an Avanti mini-extruder[14] where they passed through 1 µm-wide pores of a track-etched membrane, making the GUVs burst and reassemble around the bacteria. The block copolymer membrane not only encapsulated the bacteria but also permitted their targeted decoration with cholesterol-PEG$_4$-Cy5 (**Figure 2**a,b; Figure S1, Supporting Information). Fluorescence imaging of YFP-expressing *E. coli* showed the fluorescence of Cy5 around the bacteria (Figure 2b; Figure 2, Supporting Information), alongside a small amount of leftover polymer structures still not around the bacteria. Some insertion of cholesterol-PEG$_4$-Cy5 onto the non-coated cells could be observed. However, the amount of cholesterol-PEG$_4$-Cy5 on the cells significantly increased when coated with PL121 (Figure S1, Supporting Information). Three different polymer concentrations (w/v%; *E. coli*@0.034%, *E. coli*@0.051%, and *E. coli*@0.062%, respectively) were tested to further characterize the construct, corresponding to increasing amounts of GUVs coextruded with bacteria (Table S1, Supporting Information). Cryo-transmission electron microscopy (cryo-TEM) shows an increase of the membrane thickness of encapsulated bacteria, ranging from 4 to 9 nm, as the polymer concentration increases (Figure 2c). These values are lower than what was previously reported for the thickness of the polymer membrane of PL121 GUVs (11 nm),[20] suggesting that the membrane is not "floating" around the cell and the polymer chains on the bacterium are not stretched, but rather form a membrane made of heavily coiled polymer chains, as previously reported for block copolymers with a >2000 Da hydrophobic chain.[21] The ζ-potential of encapsulated bacteria was closer to that of GUVs than that of naked bacteria but still more electronegative (Figure 2d), whereas bacteria simply mixed with GUVs maintain a strongly electronegative ζ-potential (Figure S4, Supporting Information). During 24 h at 37 °C, the ζ-potential of the polymer-encapsulated cells decreased, most likely because of the growth of bacteria that eventually break free from their synthetic membrane. However, when the encapsulated cells were kept in the fridge for the same time, the ζ-potential drop was minimal (Figure 2d), that is, the polymer membrane stayed intact when the cells were resting at 4 °C. Moreover, when the bacteria, grown

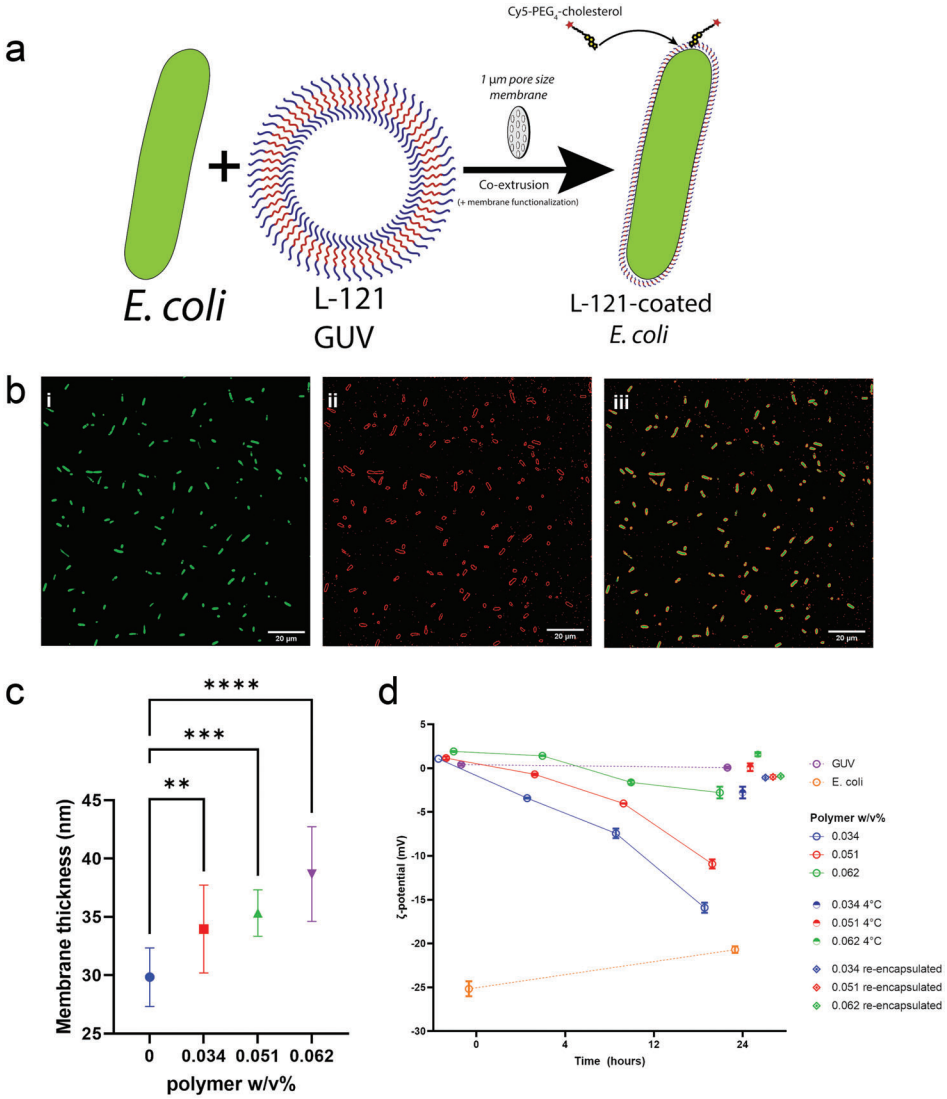


**Figure 2.** a) Concept for coating *E. coli* with PL121 by co-extrusion of the bacteria with GUVs. b) CLSM micrograph of PL121 coated bacteria (i) YFP-expressing *E. coli*; ii) Cy5-labeled polymer membrane; iii) overlay). c) Membrane thickness (cell wall + polymer) (mean ± S.D., $n = 20$ sections) measured from cryoTEM micrographs. d) $\zeta$-potential (mean ± S.D., $n = 11$) of naked and PL121 encapsulated bacteria at different w/v% and of pure GUVs, from $t = 0$ to 24 h later, either kept at 37 °C (empty circles), 4 °C (half-empty circles), or re-encapsulated within new polymer (rhombus+dot). **: $p < 0.01$; ***: $p < 0.001$; ****: $p < 0.0001$.

for 24 h at 37 °C, were re-encapsulated, they recovered the previous $\zeta$-potential. Thus, if the polymer shell of the cells is lost during cell growth, it can be replenished by another round of co-extrusion with PL121 GUVs.

The lack of any clearly visible micro-sized domain or blotchy coating in both CLSM and cryo-TEM (Figure S3, Supporting Information) suggests—within the resolution limit of the imaging techniques—that the coating is uniform and almost completely masks the bacterium's surface charge. By staining the cells with fluorescein diacetate (FDA, live staining) and propidium iodide (PI, dead staining), we could determine that the great majority of encapsulated cells was still metabolically active (Figure S5, Supporting Information). Interestingly, cells initially showed slower growth kinetics with more polymer, but these differences were almost negligible over the course of 24 h (Figure S6, Supporting Information). The bacteria proliferated on agar independently on the encapsulation; only the highest concentration showed a limited hindrance, possibly due to more cells enwrapped by enough polymer to slow their growth (Figure S7a, Supporting Information). No damage to the bacterial membrane was detected, as plasmids were not lost over time in a plasmid retention assay (Figure S7b, Supporting Information). Overall, these results show that the bacteria were enwrapped by a thin polymeric membrane that influenced their surface features and proliferation. Compared to other multi-cell encapsulation systems, the amount of polymer needed was orders of magnitude lower than what was used to encapsulate bacteria in Pluronic-based hydrogels,[22] making SCNE a possible alternative to biofilm encapsulation, should the quantity of synthetic polymer need to be limited.

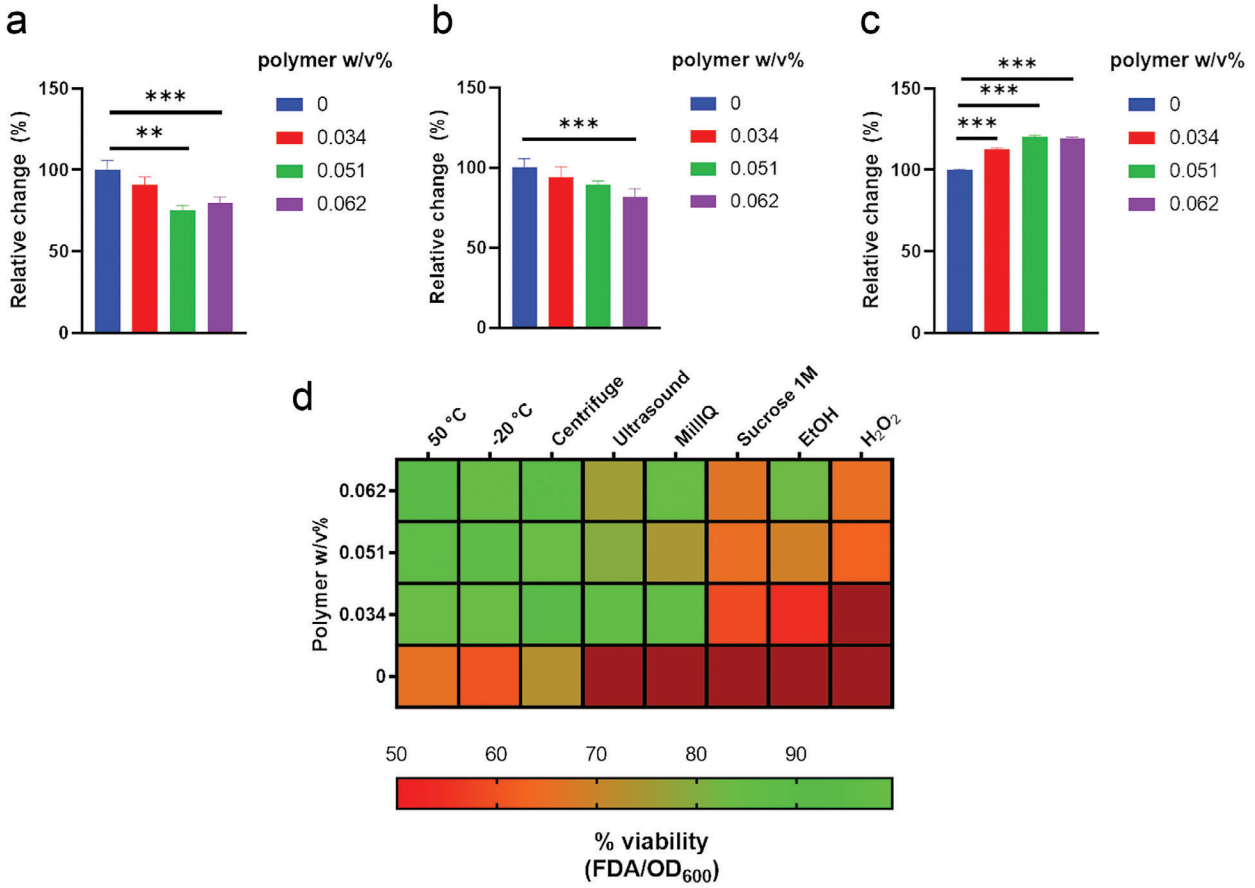


**Figure 3.** a) Relative change in FDA conversion of naked and PL121-encapsulated bacteria (mean ± S.D., $n = 3$). b) Relative change in $OD_{600}$ of naked and encapsulated bacteria (mean ± S.D., $n = 3$). c) Relative change in NAD(P)H content of naked and encapsulated bacteria (mean ± S.D., $n = 3$). d) Heatmap of the % viability (expressed as FDA conversion / $OD_{600}$) of bacteria compared to the same bacteria, encapsulated but untreated, when subjected to a selection of harsh conditions. Values below 50% were assigned dark red. The numerical values are reported in Table S2, Supporting Information. **: $p < 0.01$; ***: $p < 0.001$.

### 2.2. Cell Metabolism and Protection upon Encapsulation

Having established a protocol for encapsulating the bacteria in a thin polymer membrane, the influence of the encapsulation on the cell metabolism was investigated next. Three optically measurable biomarkers were selected: the well-known viability assay via the conversion of FDA to fluorescein (**Figure 3**a), the optical density at 600 nm ($OD_{600}$) as a measure of the bacterial growth (Figure 3b), and the fluorescence of NAD(P)H as an indication of the overall redox potential of cells (Figure 3c). For our assays, we selected a time span of 4 h, as the growth curve showed that the coated and non-coated cells grew with different kinetics, thus still being fully affected by the polymer membrane. Moreover, this time span is a good instance of shorter-time biotransformations.[23] The FDA metabolism decreased with increasing polymer concentration, most likely because the shell increased in thickness, slowing down the diffusion of the substrate to the bacteria. The $OD_{600}$ decreased with increasing polymer concentration, that is, cell division decreased, most likely because the weak mechanical constraint of the polymer membrane hindered cell division (Figure 3b). However, NAD(P)H levels increased with higher polymer concentrations, as the decreased cell proliferation meant that more reducing energy was available within the cells (Figure 3c), which is in line with results from previous cell encapsulation studies.[7b]

The encapsulation of microorganisms has been shown to protect cells from several physicochemical stressors,[4] a very beneficial feature for any industrial application. To investigate the protective effect of the PL121 membrane on the cells, encapsulated bacteria were subjected to several harsh conditions. As a viability stand-in, their FDA conversion was compared to naked bacteria in the same conditions (Figure 3d; Table S2, Supporting Information). The encapsulation in a P121 membrane increased the retention of cell viability when stressed with high and low temperatures. This was particularly pronounced (99% viability) at lower polymer concentrations, possibly due to temperature-dependent modifications of Pluronic packing and permeability, inducing the collapse and compaction of chains.[24] The polymer shell also protected the bacteria against mechanical stresses, such as high-speed centrifugation and ultrasonication. When subjected to osmotic stress, polymer-enwrapped cells were more protected than their naked counterparts if put in a hypoosmotic environment (MilliQ water). In contrast, the improvement was remarkably smaller for a hyperosmotic medium (1 M sucrose,

38% viability for naked cells to a maximum of 66% when encapsulated), evidencing that the polymer membrane could withstand cell swelling, but was unable to help against cell shrinkage. Against chemical agents (70% EtOH and 20% $H_2O_2$, respectively), a thicker shell provided better protection, most likely because it limited the diffusion of the chemical agents to the cell.

For comparison, bacteria were mixed with GUVs but not coextruded and subjected to the same stressful conditions. The simple presence of the GUVs improved viability only slightly (Figure S9 and Table S3, Supporting Information), indicating that the polymer has to form a membrane around the bacteria to protect them efficiently. Similarly, bacteria growing out of their membranes (incubated at 37 °C) withstood less efficiently the harsh conditions than those kept at 4 °C (Figure S9 and Table S3, Supporting Information).

Having demonstrated the protective effect of the polymer coating, we moved on to a more complex model application, where an engineered whole-cell biocatalyst (WCB) would be stressed with several temperature shocks, that is, simulating mishandled storage conditions or multi-step reaction cycles. The possibility of inducing protein production in the polymer-coated bacteria was confirmed (Figure S8, Supporting Information). Then, myoglobin (Mb)-producing bacteria were coated with the polymer and subjected to a heat-cold-heat cycle. The coated WCBs were washed, resuspended in new medium, and Mb expression was induced. The peroxidase activity of Mb was confirmed by the production of ABTS radicals (Figure S10, Supporting Information) and by luminescence occurring from the oxidation of luminol (Figure 3; Figure S11, Supporting Information).[25] While untreated, naked bacteria had a catalytic advantage against encapsulated *E. coli*@0.062% bacteria, they lost their activity once subjected to the harsh heat-cold-heat treatment. In contrast, the encapsulated Mb-expressing bacteria only suffered a minor decrease in catalytic activity (**Figure** 4b). Finally, we applied the coating's protection against chemical agents to a model WCB detoxification process using the dehalogenation activity of peroxidases. Mb-producing bacteria were used to convert the mutagenic and carcinogenic 2,4,6-trichlorophenol (2,4,6-TCP) to its less toxic hydroxyquinone (Figure S12a, Supporting Information)[26] using $H_2O_2$, which was either added directly or produced in situ by glucose oxidase. By monitoring the absorbance of 2,4,6-TCP (Figure S12b, Supporting Information), of the intermediate 2,6-dichloroquinone (2,6-DCQOH) (Figure S12c, Supporting Information), and of the end product 2,6-dichlorohydroxyquinone (2,6-DCQOH) (Figure S12d, Supporting Information), we could progressively observe the conversion of 2,4,6-TCP to 2,6-DCQOH. The experiments demonstrated a synergy between encapsulation and the slow in situ production of $H_2O_2$ that allowed the bacteria to detoxify their medium and increase their biomass. When $H_2O_2$ was added as in a single shot, bacteria had hindered proliferation than when GOX gradually provided it. However, even in this case, encapsulated bacteria survived more easily than naked ones (Figure S12e, Supporting Information).

The polymer membrane on the bacteria also protects the cells from macromolecular degrading agents, namely the bacteriolytic lysozyme. Gram-negative *E. coli* is susceptible to this hydrolase enzyme. The membrane made the bacteria more resistant (Figure 4c). As the polymer concentration increased, the advantage over naked bacteria with higher concentrations of lysozyme increased, reaching an eightfold improvement in bacterial vitality for the highest concentration of enzyme with the highest concentration of polymer (Figure 4d). This resistance to lysozyme was applied to a model of a culture contamination, where lysozyme might be used to selectively eliminate unencapsulated bacteria (the contaminant) while encapsulated ones should be retained. To test this hypothesis, non-fluorescent unencapsulated bacteria were mixed with the same strain enwrapped in polymer and that expressed yellow fluorescent protein (YFP). As unencapsulated bacteria can grow unhindered by the encapsulation, they will tend to outgrow their fluorescent counterparts. Thus, the ratio between fluorescent signal (only one population) and $OD_{600}$ (both populations) will decrease over time. A selective antimicrobial, such as lysozyme, can counter this phenomenon (Figure 4e). When unencapsulated bacteria were mixed in a 10:1 ratio to encapsulated ones, we could observe how the YFP/$OD_{600}$ ratio would quickly drop over time in the absence of lysozyme. However, it remained constant in the presence of lysozyme (Figure 4f). Moreover, the resulting cell debris confirmed lysozyme's action (Figure S13, Supporting Information). If we prepared a 100:1 population ratio instead, the lysozyme could not stop the outgrowth of unencapsulated bacteria but slowed it down markedly (Figure 4g). Thus, the polymer membrane selectively protected the encapsulated bacteria and could be used, in combination with externally added lysozyme, to remove unwanted microbes.

### 2.3. Membrane Decoration with Exoenzymes

The polymer membrane does not only protect the cells, but it also offers a convenient anchor for surface decoration with various molecules. One example was the insertion of Cy5 to label the membrane via its conjugation to a cholesterol-$PEG_4$ anchor. Moreover, cholesterol that bears clickable moieties allows to modify the bacteria's new membrane easily, and thus the surface of the polymer-encapsulated bacteria, with a wide array of interesting biomolecules.[18,27] One possibility is the functionalization of the cell surface with non-native exoenzymes, effectively modifying their surface reactivity without the need for genetic engineering.[28] For instance, *E. coli* does not excrete $\alpha$-amylase ($\alpha$AM),[29] an enzyme that digests starch to maltose. By conjugating $\alpha$AM to cholesterol-$PEG_4$, followed by cholesterol insertion into the encapsulating membrane, the surface of the polymer-encapsulated bacteria was decorated with the enzyme, allowing *E. coli* to proliferate on starch alone (**Figure 5**a). Encapsulated bacteria without amylase grew less than naked ones without amylase and slightly better in the presence of free amylase. However, if the encapsulated bacteria were decorated with $\alpha$AM-cholesterol, their growth improved compared to naked ones. Thus, the enzyme on the surface readily delivered maltose to the cells. The cells were centrifuged and washed to remove any $\alpha$AM not attached to the polymer membrane. Without cholesterol, encapsulated cells performed worse again than the naked ones, whereas polymer-enwrapped bacteria modified with cholesterol-$PEG_4$-$\alpha$AM retained most of their viability (Figure 5b). These results confirmed that the synergy between an additional membrane and an exoenzyme

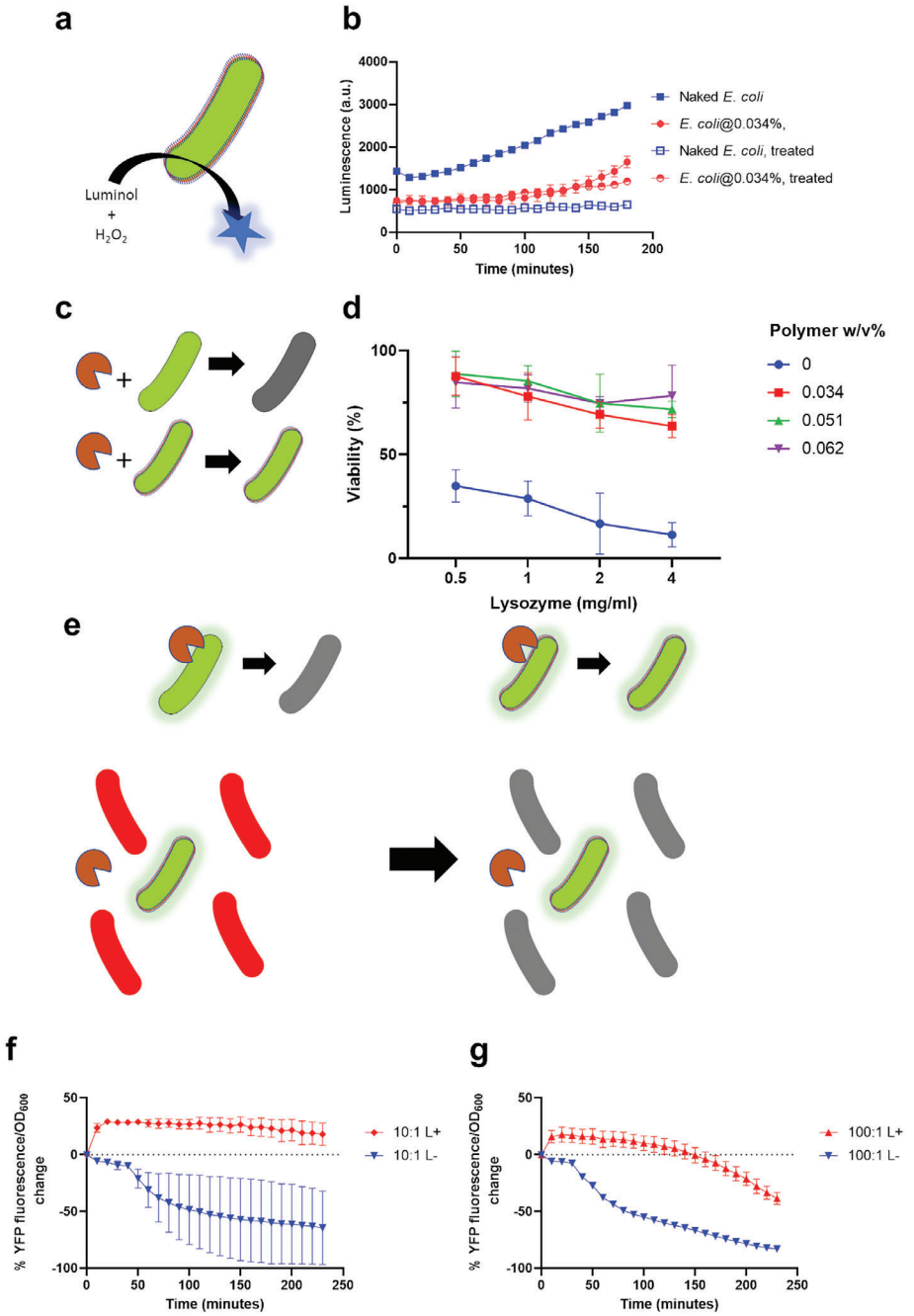


**Figure 4.** a) Schematic of luminescence production via Mb-expressing bacteria. b) Luminescence profile of naked and encapsulated Mb-producing bacteria (*E. coli*@0.034%), as base activity and after treatment with a series of temperature and mechanical shocks (mean ± S.D., $n = 3$). c) Schematic of the effect of lysozyme on naked and PL121 encapsulated bacteria. d) Viability (FDA/$OD_{600}$ compared to naked, untreated bacteria) of encapsulated bacteria when exposed to increasing concentrations of lysozyme (mean ± S.D., $n = 3$) over 4 h. e) Schematic of the action of lysozyme on naked, non-fluorescent bacteria and encapsulated, fluorescent bacteria (*E. coli*@0.062%) and of the YFP/$OD_{600}$ assay to evaluate the discriminating activity of lysozyme in mixed populations. f) YFP/$OD_{600}$ profile in a mixed population (10:1 naked:encapsulated) with (L+) and without (L−) lysozyme (mean ± S.D., $n = 3$). g) YFP/$OD_{600}$ profile in a mixed population (100:1 naked:encapsulated) with (L+) and without (L−) lysozyme (mean ± S.D., $n = 3$).

with cholesterol endowed the bacteria with a novel metabolic capability.

Carbohydrate digestion was not the only possibility, however. In nature, some bacteria, such as *Bdellovibrio bacteriovorus*, prey on other bacterial species, including pathogenic ones, and are thus being researched as interesting antibiotic alternatives.[30] Inspired by this kind of bacteria, we modified cholesterol-$PEG_4$ with lysozyme and decorated the surface of polymer-enwrapped *E. coli* with it (Figure 5c). In this way, the bacteria become armed with a molecule that kills their unarmored equivalents.

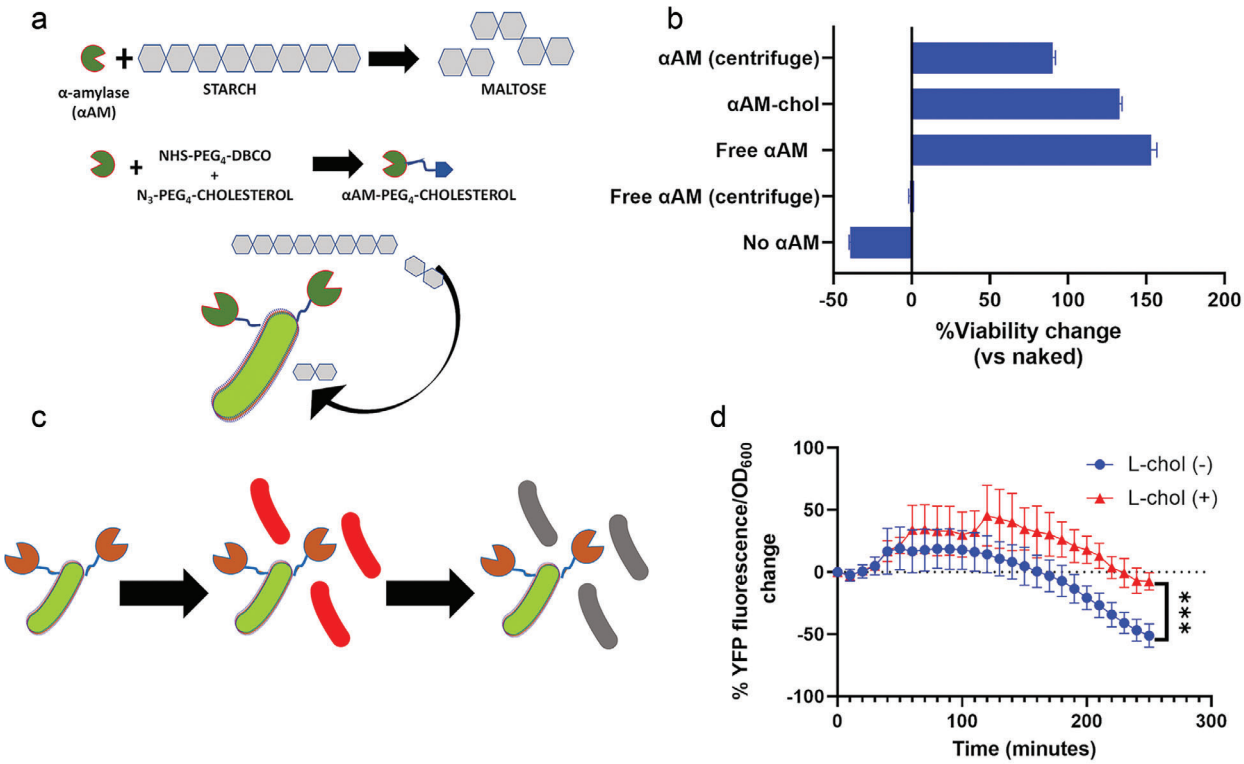


**Figure 5.** a) Schematic of the mechanism of $\alpha$-amylase ($\alpha$AM) and its functionalization onto the surface of bacteria, allowing digestion of starch by *E. coli*@0.62%, after 4 h. b) Viability change (FDA fluorescence) of encapsulated and naked bacteria growing on starch alone, with $\alpha$AM in solution (free) or $\alpha$AM on their surface ($\alpha$AM-chol) (mean ± S.D., $n = 3$). Controls include bacteria with free $\alpha$AM after a washing step to remove it and bacteria with no enzyme at all. c) Schematic of the functionalization of lysozyme onto the surface of bacteria and its action against naked bacteria. d) Variation of YFP/$OD_{600}$ profile overtime for a mixed population of encapsulated, fluorescent and lysozyme-equipped bacteria (L-chol (+)) and naked bacteria, showing the slowing down of outgrowth of the latter by the former over 4 h (mean ± S.D., $n = 3$). ***: $p < 0.001$.

Surface-functionalized fluorescent bacteria were mixed with naked, non-fluorescent ones. The ratio between fluorescence and $OD_{600}$ is an indicator of the encapsulated bacteria fraction in the culture. It dropped quickly in the absence of lysozyme (i.e., the naked bacteria grow faster). Still, it was slower to decrease when the encapsulated bacteria were equipped with the enzyme on their surface and could counteract the others' growth (Figure 5d). However, the ratio eventually decreased in this case, too, over 4 h, indicating that the surface-bound lysozyme could not easily reach other bacteria, relying instead on two bacteria being close enough for the lysozyme to act and kill the other bacteria.

## 3. Conclusion

We have developed a simple single-cell encapsulation process using amphiphilic block copolymers that form a thin cell-wall-like structure around individual cells. This allowed *E. coli* to resist a wide array of degrading agents and protected it against hydrolytic enzymes that, therefore, selectively inactivated non-encapsulated bacteria. Moreover, the block copolymer membrane acted as an anchor for surface modifications of the bacteria with exoenzymes, allowing the bacteria to grow on non-canonical macromolecular nutrients or to become predators with the ability to kill their unencapsulated counterparts. Thus, encapsulation of bacterial cells with an amphiphilic block copolymer membrane and surface functionalization of this synthetic layer allows changing the phenotype of cells, making them able to withstand various cell-toxic agents and physical stresses without any genotype modification. Like any cell surface engineering and cell encapsulation with synthetic polymers, the encapsulation method presented herein is not self-replicating. Thus, growing cell populations will lose the protective effect of the polymer over time. However, the effects of the polymer encapsulation last long enough to conduct, for example, useful whole-cell biotransformations, the polymer membrane can be easily regained by another round of co-extrusion with PL121 GUVs, and the cells keep the protective polymer coating when resting at 4 °C. Thus, the bio-inspired coating could find applications in industrial and environmental biotechnology, for example, to allow the use of WCBs in previously unfavorable environments. Moreover, polymer-enwrapped cells could also be useful in biomedical research, synthetic biology and for engineered living materials, as the easy functionalization of their surface consents the decoration with a plethora of molecules, with applications ranging from targeting to surface adhesion, exocellular catalysis and selective killing.

## Supporting Information

Supporting Information is available from the Wiley Online Library or from the author.

## Acknowledgements

This project received funding from the European Union's Horizon 2020 research and innovation program under the Marie Skłodowska-Curie grant agreement No. 101032493. I.H. acknowledges support from the EU SuperCol Project under grant agreement No. 860914. The authors wish to acknowledge Dr. Brigitte Hertel for her help in electron microscopy characterization, Prof. Wolf-Dieter Fessner for the provided strain, Dr. Aaron K. Lau for providing access to his facility, and Michael Kickstein and Eleonora Ornati for assistance with bacterial cultures. The authors acknowledge the funding provided by ULB Darmstadt for publication.

Open access funding enabled and organized by Projekt DEAL.

## Conflict of Interest

The authors declare no conflict of interest.

## Data Availability Statement

The data that support the findings of this study are available from the corresponding author upon reasonable request.

## Keywords

block copolymers, cytoprotection, membrane functionalization, membranes, single-cell encapsulation

Received: April 25, 2023
Revised: July 6, 2023
Published online: July 14, 2023

[1] K. J. D. Lee, S. E. Marcus, J. P. Knox, *Mol. Plant* **2011**, *4*, 212.
[2] a) V. Krzyzanek, N. Sporenberg, U. Keller, J. Guddorf, R. Reichelt, M. Schönhoff, *Soft Matter* **2011**, *7*, 7034; b) J. Gaitzsch, X. Huang, B. Voit, *Chem. Rev.* **2016**, *116*, 1053; c) M. V. Zyuzin, A. S. Timin, G. B. Sukhorukov, *Langmuir* **2019**, *35*, 4747; d) C. B. Giuliano, N. Cvjetan, J. Ayache, P. Walde, *ChemSystemsChem* **2021**, *3*, 2000049.
[3] a) H. G. Sundararaghavan, J. A. Burdick, in *Comprehensive Biomaterials* (Ed.: P. Ducheyne), Elsevier, Oxford, **2011**, pp. 115–130; b) A. Rodrigo-Navarro, S. Sankaran, M. J. Dalby, A. del Campo, M. Salmeron-Sanchez, *Nat. Rev. Mater.* **2021**, *6*, 1175.
[4] H. Lee, N. Kim, H. B. Rheem, B. J. Kim, J. H. Park, I. S. Choi, *Adv. Healthcare Mater.* **2021**, *10*, 2100347.
[5] J. J. Huang, in *Retinal Pharmacotherapy* (Eds.: Q. D. Nguyen, E. B. Rodrigues, M. E. Farah, W. F. Mieler), W.B. Saunders, Edinburgh, **2010**, pp. 81–85.
[6] a) J. Lu, W. Peng, Y. Lv, Y. Jiang, B. Xu, W. Zhang, J. Zhou, W. Dong, F. Xin, M. Jiang, *Ind. Eng. Chem. Res.* **2020**, *59*, 17026; b) I. Moya-Ramírez, P. Kotidis, M. Marbiah, J. Kim, C. Kontoravdi, K. Polizzi, *ACS Synth. Biol.* **2022**, *11*, 1303.
[7] a) T. G. Johnston, S.-F. Yuan, J. M. Wagner, X. Yi, A. Saha, P. Smith, A. Nelson, H. S. Alper, *Nat. Commun.* **2020**, *11*, 563; b) H. Priks, T. Butelmann, A. Illarionov, T. G. Johnston, C. Fellin, T. Tamm, A. Nelson, R. Kumar, P.-J. Lahtvee, *ACS Appl. Biol. Mater.* **2020**, *3*, 4273.
[8] F. Shao, L. Yu, Y. Zhang, C. An, H. Zhang, Y. Zhang, Y. Xiong, H. Wang, *Front. Bioeng. Biotechnol.* **2020**, *8*.
[9] S. D. Ling, Y. Geng, A. Chen, Y. Du, J. Xu, *Biomicrofluidics* **2020**, *14*, 061508.
[10] D. Vona, S. R. Cicco, R. Ragni, C. Vicente-Garcia, G. Leone, M. M. Giangregorio, F. Palumbo, E. Altamura, G. M. Farinola, *Photochem. Photobiol. Sci.* **2022**, *21*, 949.
[11] a) S. S. Balkundi, N. G. Veerabadran, D. M. Eby, G. R. Johnson, Y. M. Lvov, *Langmuir* **2009**, *25*, 14011; b) Y. J. Eun, A. S. Utada, M. F. Copeland, S. Takeuchi, D. B. Weibel, *ACS Chem. Biol.* **2011**, *6*, 260; c) R.-B. Song, Y. Wu, Z.-Q. Lin, J. Xie, C. H. Tan, J. S. C. Loo, B. Cao, J.-R. Zhang, J.-J. Zhu, Q. Zhang, *Angew. Chem., Int. Ed.* **2017**, *56*, 10516; d) T. Harimoto, J. Hahn, Y.-Y. Chen, J. Im, J. Zhang, N. Hou, F. Li, C. Coker, K. Gray, N. Harr, S. Chowdhury, K. Pu, C. Nimura, N. Arpaia, K. W. Leong, T. Danino, *Nat. Biotechnol.* **2022**, *40*, 1250; e) S. Peil, S. J. Beckers, J. Fischer, F. R. Wurm, *Mater. Today Biol.* **2020**, *7*, 100061; f) J. Pan, G. Gong, Q. Wang, J. Shang, Y. He, C. Catania, D. Birnbaum, Y. Li, Z. Jia, Y. Zhang, N. S. Joshi, J. Guo, *Nat. Commun.* **2022**, *13*, 2117.
[12] a) L. Wang, Y. Li, X.-Y. Yang, B.-B. Zhang, N. Ninane, H. J. Busscher, Z.-Y. Hu, C. Delneuville, N. Jiang, H. Xie, G. Van Tendeloo, T. Hasan, B.-L. Su, *Natl. Sci. Rev.* **2021**, *8*, nwaa097; b) H. Lee, J. Park, N. Kim, W. Youn, G. Yun, S. Y. Han, D. T. Nguyen, I. S. Choi, *Adv. Mater.* **2022**, *34*, 2201247.
[13] J. Li, C. Zheng, B. Liu, T. Chou, Y. Kim, S. Qiu, J. Li, W. Yan, J. Fu, *Nanotechnology* **2018**, *29*, 365705.
[14] Z. Cao, S. Cheng, X. Wang, Y. Pang, J. Liu, *Nat. Commun.* **2019**, *10*, 3452.
[15] a) A. M. Bodratti, P. Alexandridis, *Expert Opin. Drug Delivery* **2018**, *15*, 1085; b) M. G. Gouveia, J. P. Wesseler, J. Ramaekers, C. Weder, P. B. V. Scholten, N. Bruns, *Chem. Soc. Rev.* **2023**, *52*, 728.
[16] T. Foster, K. D. Dorfman, H. T. Davis, *Langmuir* **2010**, *26*, 9666.
[17] M. Houbrechts, L. Caire da Silva, A. Ethirajan, K. Landfester, *Soft Matter* **2021**, *17*, 4942.
[18] R. Luo, K. Göpfrich, I. Platzman, J. P. Spatz, *Adv. Funct. Mater.* **2020**, *30*, 2003480.
[19] A. Belluati, V. Mikhalevich, S. Yorulmaz Avsar, D. Daubian, I. Craciun, M. Chami, W. P. Meier, C. G. Palivan, *Biomacromolecules* **2020**, *21*, 701.
[20] D. F. do Nascimento, L. R. Arriaga, M. Eggersdorfer, R. Ziblat, M. d. F. V. Marques, F. Reynaud, S. A. Koehler, D. A. Weitz, *Langmuir* **2016**, *32*, 5350.
[21] F. Itel, M. Chami, A. Najer, S. Lörcher, D. Wu, I. A. Dinu, W. Meier, *Macromolecules* **2014**, *47*, 7588.
[22] S. Bhusari, S. Sankaran, A. del Campo, *Adv. Sci.* **2022**, *9*, 2106026.
[23] a) B. Lin, Y. Tao, *Microb. Cell Fact.* **2017**, *16*, 106; b) K. N. Schwaiger, A. Voit, B. Wiltschi, B. Nidetzky, *Microb. Cell Fact.* **2022**, *21*, 61.
[24] P. Alexandridis, T. Nivaggioli, T. A. Hatton, *Langmuir* **1995**, *11*, 1468.
[25] Z. Song, L. Wang, S. Hou, *Anal. Bioanal. Chem.* **2004**, *378*, 529.
[26] a) Z. Pan, Z. Du, J. Jia, A. Lin, Y. Wang, W. Song, S. Sun, H. Wang, R. Jia, L. Hou, *Chemosphere* **2022**, *296*, 134014; b) S. Franzen, K. Sasan, B. E. Sturgeon, B. J. Lyon, B. J. Battenburg, H. Gracz, R. Dumariah, R. Ghiladi, *J. Phys. Chem. B* **2012**, *116*, 1666.
[27] K. A. Davis, P.-J. Wu, C. F. Cahall, C. Li, A. Gottipati, B. J. Berron, *J. Biol. Eng.* **2019**, *13*, 5.
[28] a) V. Maffeis, A. Belluati, I. Craciun, D. Wu, S. Novak, C.-A. Schoenenberger, C. G. Palivan, *Chem. Sci.* **2021**, *12*, 12274; b) A. Belluati, I. Craciun, C. G. Palivan, *ACS Nano* **2020**, *14*, 12101; c) A. Belluati, I. Craciun, J. Liu, C. G. Palivan, *Biomacromolecules* **2018**, *19*, 4023.
[29] a) M. Raha, I. Kawagishi, V. Müller, M. Kihara, R. M. Macnab, *J. Bacteriol.* **1992**, *174*, 6644; b) J. K. Roy, A. Borah, C. L. Mahanta, A. K. Mukherjee, *J. Mol. Catal. B: Enzym.* **2013**, *97*, 118.
[30] a) R. J. Atterbury, J. Tyson, *Microbiology* **2021**, *167*; b) C. J. Harding, S. G. Huwiler, H. Somers, C. Lambert, L. J. Ray, R. Till, G. Taylor, P. J. Moynihan, R. E. Sockett, A. L. Lovering, *Nat. Commun.* **2020**, *11*, 4817.